Article

Atomic Resolution Density Maps Reveal Secondary Structure Dependent Differences in Electronic Distribution

Paula I. Lario, and Alice Vrielink

J. Am. Chem. Soc., **2003**, 125 (42), 12787-12794• DOI: 10.1021/ja0289954 • Publication Date (Web): 25 September 2003

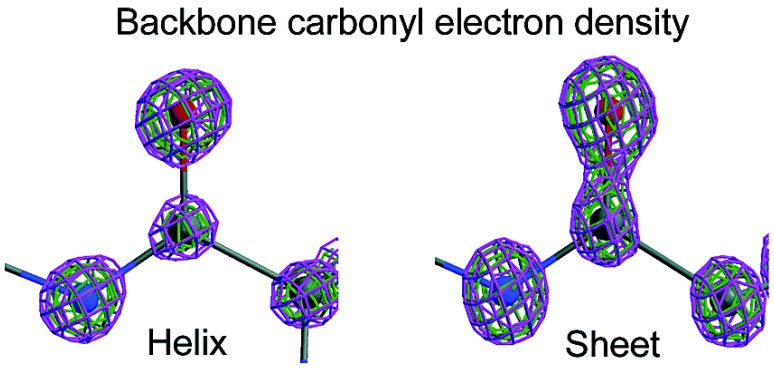

More About This Article

Additional resources and features associated with this article are available within the HTML version:

- Supporting Information
- Links to the 2 articles that cite this article, as of the time of this article download
- Access to high resolution figures
- Links to articles and content related to this article
- Copyright permission to reproduce figures and/or text from this article

View the Full Text HTML

J|A|C|S
ARTICLES
Published on Web 09/25/2003

Atomic Resolution Density Maps Reveal Secondary Structure Dependent Differences in Electronic Distribution

Paula I. Lario and Alice Vrielink*

Contribution from the Department of Molecular, Cellular and Developmental Biology & Department of Chemistry and Biochemistry, Sinsheimer Laboratory, University of California Santa Cruz, Santa Cruz, CA, 95064, Biochemistry Department, McGill University, Montréal, QC, H3G-1Y6.

Received October 17, 2002; E-mail: vrielink@biology.ucsc.edu

Abstract: The X-ray crystal structure of the flavoenzyme cholesterol oxidase, SCOA (*Streptomyces sp.*SA-COO) has been determined to 0.95 Å resolution. The large size (55kDa) and the high-resolution diffraction of this protein provides a unique opportunity to observe detailed electronic effects within a protein environment and to obtain a larger sampling for which to analyze these electronic and structural differences. It is well-known through spectroscopic methods that peptide carbonyl groups are polarized in α-helices. This electronic characteristic is evident in the sub-Ångstrom electron density of SCOA. Our analysis indicates an increased tendency for the electron density of the main chain carbonyl groups within α-helices to be polarized toward the oxygen atoms. In contrast, the carbonyl groups in β-sheet structures tend to exhibit a greater charge density between the carbon and oxygen atoms. Interestingly, the electronic differences observed at the carbonyl groups do not appear to be correlated to the bond distance of the peptide bond or the peptide planarity. This study gives important insight into the electronic effects of α-helix dipoles in enzymes and provides experimentally based observations that have not been previously characterized in protein structure.

Introduction

Carbonyl groups are perhaps one of the most important functional groups in organic chemistry. The reactivity of a carbonyl group depends on both its substituents and its surrounding environment. For instance, the electronic field generated by an α-helix in acyl-cysteine proteases, polarizes the reactive carbonyl group of the substrate thus increasing its reactivity toward nucleophilic attack.[1] An α-helix dipole has been proposed to facilitate the oxidation reaction in cholesterol oxidase and other flavin oxidases such as D-amino acid oxidase, by stabilizing the additional negative charge generated on the reduced flavin cofactor.[2−4] Direct visualization of the electronic environments of backbone carbonyl groups within different structural elements will help in understanding the effects of electronic properties within a protein. In addition, such an analysis will provide an important link between other observations, including experimental data derived from spectroscopic methods and theoretically derived parameters and will lead to an improved understanding of the electronic features of secondary structure elements within proteins.

The electronic environment of the peptide carbonyl group within a protein is dependent on secondary structure. Environmental differences between carbonyl groups in a protein are responsible for many spectroscopic differences observed within α-helix and β−sheet structure.[5] For example, distinct differences are observed in the backbone carbonyl FT-IR stretching frequencies between α-helices and β-sheets. These differences are routinely used to assign the percentages of secondary structure elements during the characterization of a protein. NMR chemical shift differences between α-helix and β-sheet structures have been associated with varying degrees of polarization of the electron density surrounding the carbonyl group.[5]

Scheme 1. Different Resonance and Ionic Forms of an Amide Group

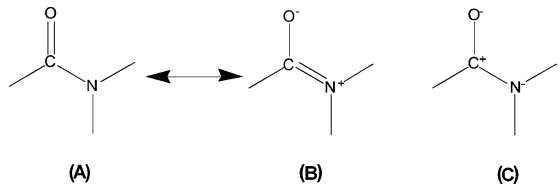

The resonance model has been used to explain the barrier to rotation around the amide bond and the general reactivity and stability of this functional group. That is, energetic stabilization is a result of π electron interactions, where charge is transferred from the lone pair on the nitrogen atom into the carbonyl π system (Scheme 1A & 1B). A systematic study of a series of twisted amide compounds was found to be consistent with the resonance model of an amide.[5] However, ab initio molecular orbital theoretical studies have lead to a new interpretation about

(1) Doran, J. D.; Carey, P. R. *Biochemistry* **1996**, *35*, 12 495−12 502.
(2) Vrielink, A.; Li, J.; Brick, P.; Blow, D. M. In *Flavins and Flavoproteins*; Curti, B., Ronchi, S., Zanetti, G., Eds.; Water de Gruyter & Co.: Berlin, 1994; pp 175−184.
(3) Ghisla, S.; Massey, V. *Eur. J. Biochem.* **1989**, *181*, 1−17.
(4) Fraaije, M. W.; Mattevi, A. *Trends Biochem. Sci.* **2000**, *25*, 126−132.
(5) Yamada, S. *J. Org. Chem.* **1996**, *61*, 941−946.

Figure 1. Backbone trace of cholesterol oxidase. Highlighted in yellow are the residues for which the carbonyl groups have been classified as sheet-share and in green are those selected as helix-gap in the analysis.

the electronic structure of amides.[6,7] Although resonance arguments are concerned with π electrons, there are also usually changes in the σ system. These changes result in amide bonds with more ionic character (Scheme 1C). Rather than a net charge transfer from the amide nitrogen atom, this electronegative atom withdraws more charge density from the carbonyl carbon atom. Thus, Coulombic interactions between atoms within the amide group play a large role in both stability and geometry. This ionic nature within an amide group has been extrapolated to account for the stability of particular secondary structure motifs in proteins.[8−10]

Macromolecular systems are unique from small molecules in that they are often composed of a significant hydrophobic core environment. Coulombic interactions are amplified in such an environment. Further studies of how carbonyl groups are affected by this microenvironment may enhance our understanding of electron polarization effects resulting from electrostatic interactions.

The sub-Ångstrom resolution refinement of cholesterol oxidase, a relatively large structurally characterized enzyme (MW = 55 kDa), has provided us with an opportunity to observe significant differences in the electron density of the amide carbonyl groups. A unique advantage of this structure is that both α-helix and β-sheet structures are well represented and are observed in varying directions throughout the structure (Figure 1). Our analysis reveals significant electronic differences in the amide carbonyl groups for cholesterol oxidase and show that these differences are correlated with secondary structure.

Methods

Cholesterol oxidase is a monomeric 55 kDa flavoenzyme that crystallizes in the monoclinic space group P21 with unit-cell parameters a = 51.273 Å, b = 72.964 Å, c = 63.036 Å, and β = 105.18°. The crystal used for this study was grown by vapor diffusion from a mother liquor containing 12% polyethylene glycol MW 8000, 75 mM $MnSO_4$, 100mM glycine buffer pH 9.0. Prior to the diffraction experiment the crystal was transferred to a cryo-protectant solution consisting of the mother liquor and 30% glycerol. Despite the presence of a pH 9.0 buffer the actual pH of the solutions used for crystallization and cryo-protection were measured to be 7.3 and 7.4, respectively. Diffraction data from the crystal cooled to 100 K was collected to a resolution of 0.95 Å at the edge and 0.92 Å to the corners of a Q4 Quantum detector on beamline X8C at the National Synchrotron Light Source, Brookhaven National Laboratory. The synchrotron radiation wavelength was 0.979 Å. The data were processed, merged and scaled with the HKL suite of software.[11] The data statistics are given in Table 1.

Table 1. Crystallographic Data and Refinement Statistics

crystal parameters:	
space group	$P2_1$
cell dimensions	a = 51.273
	b = 72.964
	c = 63.036
	β = 105.18
data collection:	
no. of measured reflections	2567129
no. of unique reflections	277783
resolution range (Å)	49 − 0.95
resolution range for the last shell (Å)	0.97 − 0.95
completeness (%)	98.8
completeness in the last shell (%)	98.8
R-merge	0.049
R-merge for the last shell	0.349
mean I/σ	19.4
mean I/σ for the last shell	2.22
refinement:	
no. of reflections used for refinement	239945
no. of reflections used for R_{free}	12008
R-factor (%)	9.7
free R-factor (%)	11.9
r.m.s (bond lengths) (Å)	0.015
r.m.s (angle distances) (Å)	0.030
no. of protein residues	499
no. of water molecules	818 (436 full)
isotropic average temperature factors (Å^2)	
all atoms	11.1
main chain atoms	7.5
side chains and waters	13.6
FAD molecule	5.6

The structure of cholesterol oxidase from *Streptomyces sp.* was previously solved and refined to 1.5 Å resolution[12] (PDB entry 1B4V). This 1.5 Å structure was used as the starting model in the crystallographic refinement. The water molecules and the FAD molecule were removed from this model and the active site residues: M122, F359, E361, H447, and N485 were all mutated to alanines. The program SHELXH-97 was used to refine both the atomic positions and the anisotropic thermal parameters.[13] Standard SHELX restraints were used for the refinement. Near the final stages of refinement the restraints were relaxed, however no further improvement in the *R*-factor was observed, indicating that there is no overall improvement in the fit of the model to the electron density. Thus, the standard restraints were applied throughout the refinement. Most aliphatic hydrogen atoms as well as all backbone hydrogen atoms were included in the model. The hydrogen atom positions were restrained to "ride" on the heteroatom to which they are bound. Multiple conformations were observed for 118 residues, including alternate loop conformations for three surface exposed loops and the divergent N-terminus and C-terminus conformations.

The free *R*-factor was monitored during the course of the refinement using a subset of 5% of the reflections randomly chosen from the total

(6) Wiberg, K. B.; Breneman, C. M. *J. Am. Chem. Soc.* **1992**, *114*, 831−840.
(7) Wiberg, K. B.; Castejon, H. *J. Org. Chem.* **1995**, *60*, 6327−6334.
(8) Maccallum, P. H.; Poet, R.; Milner-White, E. J. *J. Mol. Biol.* **1995**, *248*, 374−384.
(9) Maccallum, P. H.; Poet, R.; Milner-White, E. J. *J. Mol. Biol.* **1995**, *248*, 361−373.
(10) Milner-White, E. J. *Protein Sci.* **1997**, *6*, 2477−2482.
(11) Otwinowski, Z.; Minor, W. In *Methods in Enzymology*; Carter, C. W. J., Sweet, R. M., Eds.; Academic Press: Boston, 1997; Vol. 276, pp 307−325.
(12) Yue, Q. K.; Kass, I. J.; Sampson, N. S.; Vrielink, A. *Biochemistry* **1999**, *38*, 4277−4286.
(13) Sheldrick, G. M.; Schneider, T. R. In *Methods in Enzymology*; Carter, C. W. J., Sweet, R. M., Eds.; Academic Press: Boston, 1997; Vol. 277, pp 319−343.

diffraction data. The structure was refined to a final *R*-factor of 9.7% and a free *R*-factor of 11.9% (Table 1). All the data to 0.95 Å was used in the final refinement cycles. An additional cycle of full-matrix refinement was carried out with the restraints removed to obtain estimates of the standard deviations for atomic positions. Secondary structure assignments for the refined model were made with the program PROMOTIF.[14] The atomic coordinates and structure factor amplitudes have been deposited in the Protein Data Bank (code: 1N1P).[15]

An F_o electron density map with a grid set to 0.2 Å was calculated using SHELXPRO [13] and viewed using XTALVIEW.[16] MAPMAN [17] was used to extract and sum the electron density values at the atomic centers. The electron density values were summed for all grid points within a sphere of radius 0.6 Å around the atomic position. In addition, the density surrounding each backbone carbonyl group was examined visually at two different electron density cutoff values: 4.5 σ (3.8 e/Å^3) and 5.5 σ (4.6 e/Å^3). If no separation in the electron density surrounding the carbon and the oxygen atoms within the carbonyl group was observed at 5.5 σ, then that particular carbonyl was labeled as "share". In contrast, if the electron density surrounding the carbonyl atoms was clearly separated at 4.5 σ, the carbonyl was labeled as "gap". Carbonyl groups where a gap was observed at 5.5 σ but not at 4.5 σ were labeled as "middle".

The maximum electron density peak for an individual atom is strongly correlated to the root-mean-square (rms) deviation of the atomic position. Large atomic movements cause a smearing of the electron density thereby resulting in a lower peak density value than that for a less mobile atom. Therefore, the map cutoff values used to classify the types of carbonyl groups are only useful in comparing atoms exhibiting similar thermal displacement parameters (B-factors). Most of the backbone atoms in the structure of cholesterol oxidase exhibit low B-factors, however, as observed in many protein structures, more mobile regions of the structure are observed. In the structure of cholesterol oxidase, the average B factor for main chain atoms is 7.45 Å^2, corresponding to an average rms positional deviation of 0.385 Å. Of the 499 amino acid residues modeled in the structure of cholesterol oxidase, 152 were excluded from further study either because they exhibited thermal parameters greater than 8.0 Å^2 for the carbonyl carbon atom (124 residues) or because the backbone carbonyl group was modeled in multiple conformations (28 residues). In addition, the measured electron density for the carbonyl atoms included in the study are plotted against their respective atomic B-factors to provide a better representation of their overall density.

Results

Initial comparison of the 0.95 Å resolution electron density maps of cholesterol oxidase clearly revealed that many of the carbonyl groups within α-helices exhibit highly polarized electron density, whereas those found within β-sheet structures show a greater propensity toward a shared density between the atomic centers (Figure 2). On the basis of these observations, a more thorough analysis was carried out to confirm whether a statistically significant relationship between the electronic features for carbonyl groups could be observed for different structural elements.

As mentioned above each of the 347 residues included in the study were visually classified as either "share", "middle", or "gap" depending on the appearance of the electron density at the carbonyl centers. The "middle" region was included in order to more clearly separate the differences of the two extreme cases. An example of each of the classified carbonyl groups is shown in Figure 3. The average distribution of the classified carbonyl densities for the 347 residues included in the study (70% of the total residues) is shown in Figure 4A. With the chosen cutoff values an approximately equal distribution of the two extremes: "gap" and "share" is observed.

A comparable distribution of types of carbonyl groups was also observed for residues involved in turns, random coils or 3_{10}-helices (Figure 4B). No significant differences were observed for the carbonyl electron density between these three types of secondary structure, so these groups were pooled together and labeled as "coil". This combined "coil" group represents 54% of the residues that were included in the study. The distribution of carbonyl types for the "coil" group is similar to the average distribution observed for all 347 residues.

Only 44% of residues adopt α-helical (23%) or $\beta-$sheet structures (21%). However, clear differences for the electronic distribution of carbonyl groups between these two types of secondary structure motifs are apparent (Figure 4, parts C and D). A 14% increase relative to the average distribution of "share" type carbonyl densities within the structure is observed for carbonyls in β-sheet structures (Figure 4C) corresponding to 28 of the 72 β-sheet residues used in the analysis. In addition, an even higher percentage (29%) of "share" type carbonyl densities are observed in β-sheet structures compared to α-helical structures (compare Figure 4, parts C and D). Correspondingly, there are fewer occurrences of "gap" type carbonyl densities for $\beta-$sheet residues (8 residues of the 72 used for the analysis). Within β-sheet structures, only 11% of carbonyl groups exhibited "gap" type densities compared to the percentage of "gap" occurrences of 26% for the overall structure.

Although a predominance of "share" type carbonyl groups are observed in β-sheet structures, α-helices exhibit a significantly higher than average occurrence of "gap" type densities (Figure 4D) corresponding to 40 of the 81 α-helix residues used in the analysis. A difference of 23% was observed between carbonyl groups exhibiting a "gap" type density distribution in α-helices, and the overall distribution (compare Figure 4, parts A and D). A more pronounced difference of 38% was observed upon comparison of the gap distribution between α-helical and $\beta-$sheet structures (compare Figure 4, parts C and D).

One might expect that the observed polarization of the α-helix carbonyl groups, are associated with longer carbonyl, C═O, bond distances. A comparison of the average carbonyl bond lengths for the two extreme cases: the "gap" case within α-helices and the "share" case within β-sheets, reveal significantly longer distances within helical structures. Within cholesterol oxidase, there are 40 examples of the carbonyl groups within helices that exhibit gap type electron density and 28 examples of carbonyl groups within sheet structures that exhibit share type of density. An analysis of the average C═O bond distance within these populations is 1.244(8) Å for "gap" types within α-helices and 1.231(8) Å for the "share" types within β-sheet structures.

Despite these differences in carbonyl bond distances, here are examples of α-helix carbonyls that are of the "gap" type which have shorter C═O bond distances as well as "share" type β-sheet carbonyl groups with long C═O bond distances. For example, Glu296, present in an α-helix, has a short carbonyl

(14) Hutchinson, E. G.; Thornton, J. M. *Protein Sci.* **1996**, *5*, 212−220.
(15) Berman, H. M.; Westbrook, J.; Feng, Z.; Gilliland, G.; Bhat, T. N.; Weissig, H.; Shindyalov, I. N.; Bourne, P. E. *Nucleic Acids Res.* **2000**, *28*, 235−242.
(16) McRee, D. E. *J. Struct. Biol.* **1999**, *125*.
(17) Kleywegt, G. J.; Jones, T. A. *Acta Crystallogr. Sect. D* **1996**, *55*, 826−828.

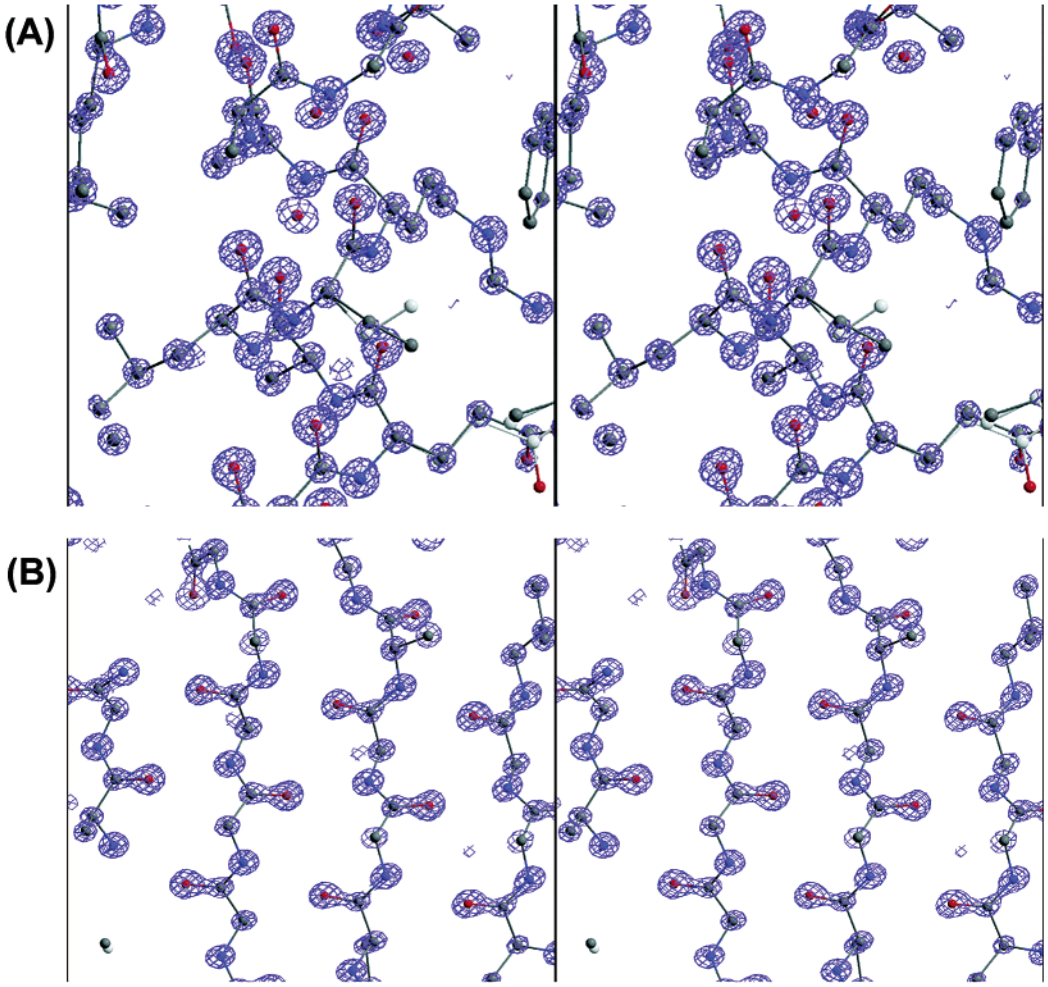

Figure 2. Stereographic representations of the electron density maps from the crystal structure of cholesterol oxidase showing (a) an α-helical region and (b) a region of β-sheet structure. The electron density maps were contoured at 4.5 σ.

bond distance (1.221(8) Å), despite the clearly polarized electron density resulting in a "gap" classification (Figure 5A). Likewise, Tyr329, present in a β-sheet, has a long carbonyl bond distance (1.253(8) Å), yet its classification as a share based on the carbonyl electron density (Figure 5B). Although both of these residues have "atypical" carbonyl bond lengths, their electron density distribution is comparable to the "typical" examples presented in Figure 3 where the carbonyl bond lengths are close to the calculated average for their respective types of secondary structure.

A further study of the geometry between the two extreme types of carbonyl groups has revealed some significant differences as well as some interesting similarities. Quite unexpectedly there were no significant differences in the average amide C−N bond distances between the gap and share type carbonyl groups, despite the observed differences in C═O bond lengths. However, differences were observed in the ranges of C−N bond distances between the two types. When comparing the C−N bond distances for the 37 examples of the sheet "share" type a slightly larger sample range was observed (0.07 Å), than for the 28 examples of the helix "gap" type (0.05 Å).

An analysis of peptide planarity was also carried out in order to determine if the classical resonance model could explain the density distribution. Although a larger deviation from planarity was observed for the O−C−N−CA dihedral angle in "share" type carbonyls within sheet structures compared to "gap" carbonyls in helical structures, there was no convincing correlation between the C−N bond distance and the dihedral angle for either type of carbonyl group. However, the average CA−C−N−CA dihedral angle was found to be closer to planarity for the "gap" type helix carbonyl groups (177(1)°) relative to the "share" type sheet groups (174(2)°).

When comparing the bond angles surrounding the carbonyl groups, we found that the average CA−C═O bond angles were essentially identical for different carbonyl types. However, for each of the other two bond angles: CA−C−N and O═C−N, differences of 2 degrees between the "gap" α-helix and "share" β-sheet carbonyl types were observed. The β−sheet "share" type carbonyl groups exhibit a larger average O═C−N bond angle (123.4(6)°) when compared to that found for α-helix "gap" type carbonyl groups (121.6(7)°). The averaged CA−C−N bond angle for the β−sheet "share" type carbonyl is 115.9(6)° and 117.9(6)° for the α-helix "gap" type. Interestingly, the 2 degree difference in the average CA−C−N bond angles between the two types is correlated to the difference in the average O═C−N bond angle suggesting a variation of the position of the nitrogen atom within the plane of the peptide bond.

This difference in the positioning of the nitrogen atom is also apparent if one compares the N−CA−C bond angle of the peptide between the two groups. The β−sheet "share" type carbonyl groups exhibit a smaller average N−CA−C bond angle (108.7(7)°) when compared to that found for α-helix "gap" type

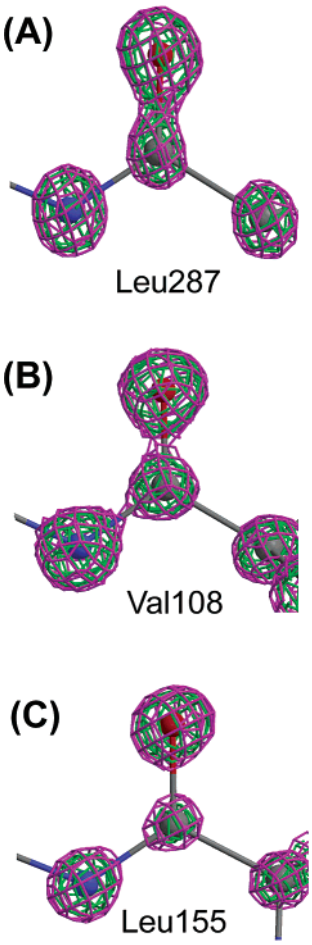

Figure 3. Peptide backbone electron density for (a) "share" (b) "middle" and (c) "gap" type carbonyl groups. Both the "share" (Leu287) and the "gap" (Leu155) type carbonyl groups represent typical examples with a carbonyl bond length representative of their respective average. The electron density maps were contoured at 4.5 σ (shown in magenta) and at 5.5 σ (shown in green).

carbonyl groups (111.0(7)°). These observations are consistent with a database analysis of oligopeptide and protein crystal structures, that have shown that the inter-peptide N−CA−C bond angle is dependent on the torsion angles of the peptide.[18,19] Ab initio (HF/4-21G) calculations have also shown torsion dependent differences in the N−CA−C bond angle for peptides.[18] Furthermore, these calculations accurately predict the large range of angles observed in oligopeptides, but do not account for the smaller range of N−CA−C bond angles observed in β-sheet and the α-helical regions in proteins.[20] Jaing and co-workers [20,21] proposed that extended peptide chains experience cooperative effects such as β-expansion and helix-compression, which result in a smaller range of N−CA−C bond angles consistent with our observations.

The polarized nature of the carbonyl density in helix "gap" type carbonyl groups as well as the increased propensity for the helix "gap" type carbonyl to be planar is consistent to the resonance model for an amide. One would expect that the

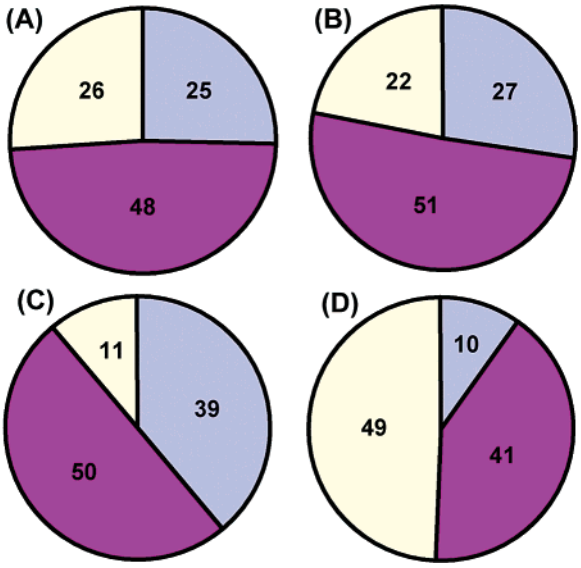

Figure 4. Electron density distribution for carbonyl groups in cholesterol oxidase. (a) Overall distribution of carbonyl types present in the enzyme (except those modeled in alternate conformations and those exhibiting thermal parameters greater than 8.0 Å^2) (b) Combined pool of the carbonyl groups found in the loop and turn regions of the structure. (c) Carbonyl groups present in β-sheet structure. (d) Carbonyl groups present in α-helical structures. blue, magenta and yellow represent carbonyl groups exhibiting "share", "middle" and "gap" type electron densities, respectively.

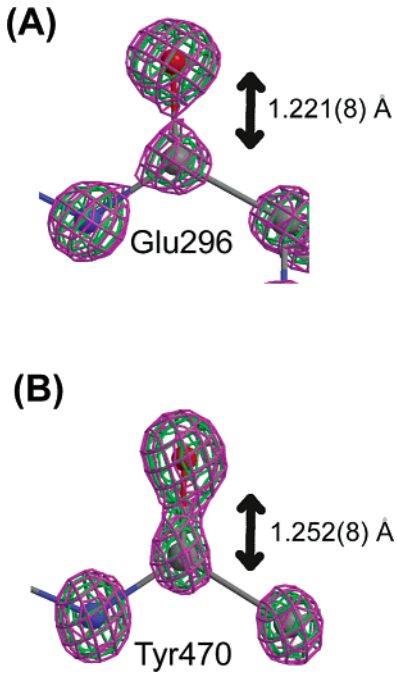

Figure 5. Peptide backbone electron density for (a) the α-helical residue, Glu296 and (b) β-sheet residue, Tyr470. Both residues have atypical carbonyl bond distances despite exhibiting the characteristic carbonyl electron density type. The electron density maps were contoured at 4.5 σ (shown in magenta) and 5.5 σ (shown in green).

oxygen atom in a polarized carbonyl group exhibits a larger partial negative charge compared to a less polarized group. To ascertain if the geometric and electronic differences observed are a result of differences in their partial charges, a comparison of the peak heights for the amide atoms in the electron density maps was carried out.

The scattering phenomena in a diffraction experiment results from the electron density within the crystal and is characterized

(18) Jiang, X.; Yu, C.-H.; Cao, M.; Newton, S. Q.; E. F., P.; Schäfer, L. *J. Mol. Struct.* **1997**, *403*, 83−93.
(19) Karplus, P. A. *Protein Sci.* **1996**, *5*, 1406−1420.
(20) Jiang, X. Q.; Cao, M.; Teppin, B.; Newton, S. Q.; Schafer, L. *J. Phys. Chem.* **1995**, *99*, 10521−10525.
(21) Van Alsenoy, C.; Yu, C.-H.; Peeters, A.; J. M. L., M.; Schäfer, L. *J. Phys. Chem. A* **1998**, *102*, 2246−2251.

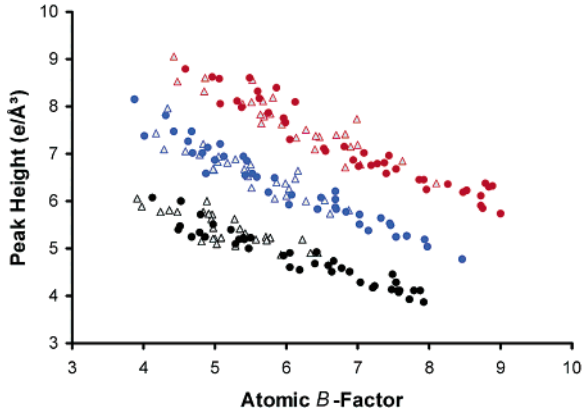

Figure 6. Atomic peak height distributions for the amide atoms present in α-helices are shown as spheres and β-sheet structure are represented as triangles. Carbon atoms are colored in black, nitrogen atoms in blue and oxygen atoms in red.

by the atomic scattering factors ($f = f_o e^{-B(\sin^2\theta)/\lambda^2}$, where f is the scattering factor for an atom at $\sin\theta/\lambda = 0$, f_o is the scattering factor at some non zero value of $\sin\theta/\lambda$ and B is related to the mean-square amplitude of atomic vibration and parameter). These scattering factors are a direct function of the atomic charge for a particular atom type and are used to calculate the electron density maps, which are based solely on the modeled structure. In addition to the atomic charge, the scattering factor is damped by an exponential function of the atomic vibration, which is not dependent on the atom type. Therefore, any observed differences in the atomic scattering factors for atoms with identical thermal parameters will be due solely to differences in their atomic charge. By comparing the integrated electron density values surrounding the atoms, any differences in atomic charge density should be apparent between atoms with similar isotropic thermal parameters. Unfortunately, during the crystallographic refinement of the structure, the atomic thermal parameters are adjusted to improve the fit of the map computed using the experimental data, to a map calculated solely on the model and pre-assigned atomic charges. Thus, the difference in the actual electron density of the atom from the pre-assigned value can be "soaked" up by the atomic thermal displacement parameters. In practice, one will observe a higher value for the thermal displacement parameters to compensate for less electron density than expected at a particular atomic position.

To obtain a more realistic view of the actual electron density around each of the atoms, the atomic peak height was plotted against the isotropic thermal displacement parameter. This graph was examined for differences in the distributions of the amide atom between the two extreme cases: the "gap" case of α-helix and the "share" cases of β−sheet carbonyl groups (Figure 6). A separation of the distributions of the two "types" of carbonyl carbon atoms is observed, where the "gap" type carbonyl carbon atom distribution is shifted both toward a lower electron density and a higher thermal parameter suggesting that less electron density is observed around these atoms in α-helical regions than in β-sheet regions of secondary structure. There are no apparent differences in the distributions for either the oxygen or the nitrogen atoms.

When using electron density cutoffs it is more evident that there is less electron density for the helix "gap" carbon atoms relative to the sheet "share" carbonyl carbon atoms. Dampening

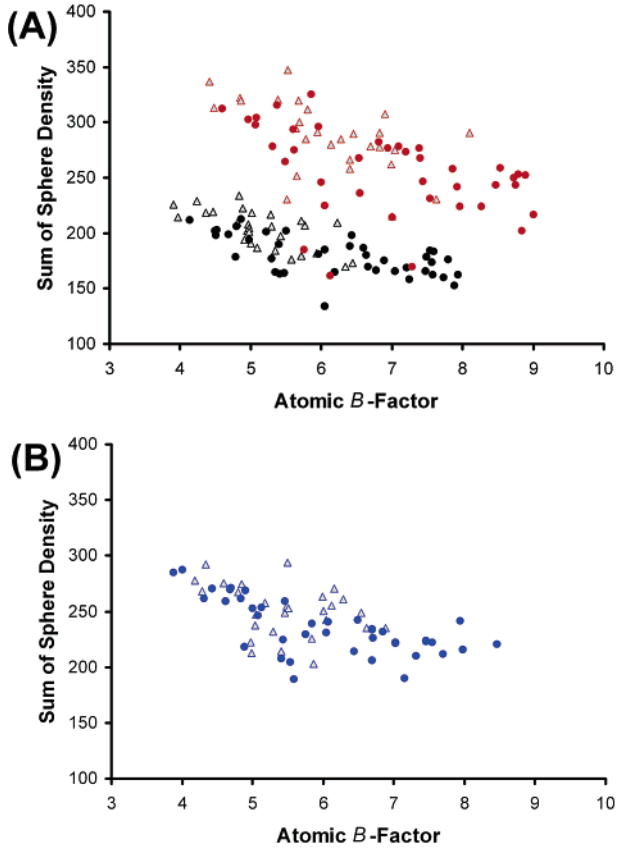

Figure 7. Electron density distributions for the amide (a) carbonyl atoms and (b) nitrogen atoms present in α-helices (●) and β-sheet structure (△). Carbon atoms are represented in black, nitrogen atoms in blue and oxygen atoms in red.

the effect of the atomic movements can be achieved by integrating the electron density in a sphere around the atom rather than comparing atomic peak heights, as the latter measurement is more sensitive to the curvature of mapped electron density.

Integrating and summing the electron density within a sphere of radius 0.6 Å surrounding the atom is more sensitive to the differences in atomic electron density than using a single grid point (at the atomic peak). This approach minimizes the errors associated with differences between a tall sharp density peak seen for a less mobile atom and the flatter density peak for a more mobile atom. When these integrated peak values were plotted against the thermal parameters the carbon atom distributions for the "gap" and "share" types are more clearly separated, with the helix "gap" carbon atom distribution shifted toward a region of lower electron density and higher thermal parameters (Figure 7A). As the thermal parameter can soak up the difference between the actual electron density and the expected electron density expected for the carbon, the distribution for the helix "gap" carbon atom indicates that there is less electron density for these carbon atoms versus the carbonyl carbon atoms located in sheet structures. Differences in the distributions for the oxygen and nitrogen atoms (Figure 7B) are not apparent with the 0.6 Å radius sphere cutoff used.

The observed electronic differences may be due to differences in hydrogen bonding geometry between the two types of secondary structure elements. An analysis of the hydrogen bonding geometry however, failed to reveal any correlation to observed differences in the electron density.

Discussion

The degree of detail that can be observed by crystallographic studies of macromolecules is limited by the attainable resolution of the diffraction pattern. The ability of electron density maps to represent the "actual" density of a molecule depends on the data resolution, data quality, and accuracy of the refined structural model. Atomic resolution data (≤ 1 Å) provides a high-quality representation of the electron density surrounding each atom of the protein and these maps easily differentiate between carbon, nitrogen and oxygen atoms for the residues with low thermal displacement parameters. One-electron differences between atom types can be correlated to the observed differences in the magnitude of the electron density around the atom. Only in a few examples have macromolecules diffracted to extremely high (sub-Ångstrom) resolution. Most of these high-resolution structures have been limited to proteins of molecular weight below 30 KDa. We present a sub-Ångstrom resolution study of a larger protein, where approximately 23% of the structure adopts α-helices and 21% adopts β-sheet structure. This provides us with an improved statistical evaluation of structural, electronic, and chemical features within a protein structure. In the past, spectroscopic methods have been used to characterize the electronic differences between backbone carbonyl groups. This study provides a unique opportunity to directly visualize differences in the electronic environment of the peptide group as a function of secondary structure elements. These results may help to clarify the relationships between the different experimental observations and the results obtained from ab initio calculations.

The calculated electron density is represented by contouring a map at various cutoff levels, where 1 σ is the average root-mean-square deviation of the noise of the map. When the electron density map for cholesterol oxidase was contoured at 4.5 σ, interesting differences in the electron density of the backbone carbonyl groups were observed (Figure 3). Originally, we noticed that many of the carbonyl groups of residues in β-sheets did not exhibit resolved electron density around the individual carbonyl atoms even when contoured at 5.5 σ. For most other atoms within the structure a 5.5 σ contour level results in well-resolved spherical electron density. This apparent delocalization of the electronic charge between the carbonyl atoms within a β-sheet could be the result of higher electron density relative to carbonyl atoms in α-helices, differences in the shapes of their "atomic" orbitals and/or differences in atomic movements. The observation of electronic differences between the two types of carbonyl groups, despite similar thermal displacement parameters indicates that the observed delocalization in β-sheet carbonyl groups is a characteristic of its environment within the protein. These electronic differences are not strictly correlated with C═O bond length since examples of both short and long carbonyl bond distances are observed for both density types; "share" and "gap"(Figures 3 and 5). As one might expect from spectroscopic studies, the carbonyl groups of residues within α-helices have a more polarized electron density than those in β-sheets (Figure 2). Indeed, analysis of our structure reveals less electron density for the carbon atoms for the α-helix carbonyl groups when compared to those in β-sheets. The predominance of a gap in the electron density between α-helix carbonyl groups contoured at 4.5 σ level suggests differences in orbital hybridization between α-helices and β-sheets.

The similar distribution of carbonyl types of the pooled "coil" structure to the overall distribution within the protein, agrees well with the calculated ^{13}CO NMR tensor distribution found for the protein, Binase, where no significant differences were observed relative to the overall average.[22] The largest differences in the tensors were found between the averaged α-helix and the β-sheet values, where the averaged isotropic chemical shift differences were σ_{iso} 178.1(1.4) for α-helix and 174.9(1.4) for β-sheet structures. These results agree well with the electronic differences observed for the carbonyl groups of cholesterol oxidase, where the α-helix carbonyl charge density is more polarized and less charge density is observed on the carbonyl carbon atom.

This polarization of the α-helix "gap" type carbonyl, does not appear to be the result of differences in the amide bond order or planarity since no significant differences in the C−N bond lengths or the C−O−N−C_a dihedral angle was observed between the carbonyl groups from different secondary structure regions. In addition, the charge density at the amide nitrogen center and within an 0.6 Å radius sphere does not indicate any dependence on the adopted secondary structure. Thus, it appears that environmental factors affecting the electron density of the carbonyl group are not associated with electronic differences of the amide nitrogen atoms. Rather, hydrogen-bonding interactions with the carbonyl group may be responsible for polarizing its electron density. However, analyses of the hydrogen bonding interactions between these two extreme types did not indicate any noticeable differences that could account for the differences in the carbonyl electron density, suggesting that perhaps other electrostatic dipole interactions are responsible. Carbonyl-carbonyl, interactions have been implicated as a significant attractive force in holding main-chain amide groups together in proteins, resulting in the predominance of particular secondary structure motifs.[8,9] The electrostatic interaction between oppositely charged oxygen and carbon atoms of carbonyl groups are proposed to be partially responsible for distorting the amide hydrogen bond geometry from planarity. The uncorrelated relationships between the C═O and C−N bond distances and the amide twist angle support such an alternative stabilizing interaction as responsible for the differences in the carbonyl electron density as opposed to the more classical resonance model. If the increased density observed for the β−sheet carbonyl carbon atom (Figure 7A) was due to donation from the lone pair nitrogen, then a decrease in density for the nitrogen atoms from β−sheet residues (Figure 7B) would be expected. Clearly, these studies indicate that the observed electronic features cannot be explained by differences in amide resonance structures.

In summary, our study suggests that, in a protein structure, the ionic nature of a planar amide (Scheme 1C) proposed by Wiberg[23] appears to be a superior model to the resonance model historically used to describe a planar peptide group. Although α-helix carbonyl bonds are slightly longer than those found in β-structure, there is no correlation between the carbonyl bond length and amide C−N bond distance. In addition, the electron density of the carbon atom for the polarized α-helix carbonyl

(22) Pang, X.; Zuiderweg, E. R. P. *J. Am. Chem. Soc.* **2000**, *122*, 4841−4842.
(23) Wiberg, K. B. *Acc. Chem. Res.* **1999**, *32*, 922−929.

is typically lower than that observed for the β-sheet carbonyl. This suggests that, for an α-helix peptide, there is less charge transfer from the nitrogen to the carbon atom despite the tendency to be more planar than β-sheet peptides.

These observations may help address our understanding of how atomic positions are related to their surrounding electronic environment, and if the strength of a bonding interaction is less dependent on distance than on the orbital shape and charge density. Further work to correlate these findings to both spectroscopic measurements and quantum mechanical calculations will help to test the accuracy and predictability of these methods to represent charge polarization within protein structure.

Acknowledgment. We thank Louis Lim, Nicole Sampson, Bill Scott, and Glenn Millhauser for useful discussions. We also thank Nicole Sampson for providing purified cholesterol oxidase for this study. This work is supported by the grants from the National Institutes of Health Grant GM63262 and the Canadian Institutes of Health Research Grant MT-13341.

JA0289954